Received: 9 January 2018 | Accepted: 1 February 2018

DOI: 10.1111/cpr.12450

ORIGINAL ARTICLE

WILEY Cell Proliferation

Overcoming resistance to mitochondrial apoptosis by BZML-induced mitotic catastrophe is enhanced by inhibition of autophagy in A549/Taxol cells

Zhaoshi Bai[1] | Meiqi Gao[1] | Xiaobo Xu[1] | Huijuan Zhang[1] | Jingwen Xu[1] | Qi Guan[2] | Qing Wang[2] | Jianan Du[1] | Zhengqiang Li[1] | Daiying Zuo[1] | Weige Zhang[2] | Yingliang Wu[1]

[1]Department of Pharmacology, Shenyang Pharmaceutical University, Shenyang, China

[2]Key Laboratory of Structure-Based Drug Design and Discovery, Ministry of Education, Shenyang Pharmaceutical University, Shenyang, China

Correspondence
Daiying Zuo, Department of Pharmacology, Shenyang Pharmaceutical University, Shenyang, China.
Email: zuodaiying@163.com

Weige Zhang, Key Laboratory of Structure-Based Drug Design and Discovery, Ministry of Education, Shenyang Pharmaceutical University, Shenyang, China.
Email: zhangweige2000@sina.com
and
Yingliang Wu, Department of Pharmacology, Shenyang Pharmaceutical University, Shenyang, China.
Email: yingliang_1016@163.com

Funding information
National Natural Science Foundation of China, Grant/Award Number: 8160130989 and 8167130571; Young and middle age backbone personnel training programme of Shenyang Pharmaceutical University, Grant/Award Number: ZQN2015003; Doctoral Scientific Research Foundation of Liaoning Province, Grant/Award Number: 201601144; Education Foundation of Liaoning Province, Grant/Award Number: 201610163L12

Abstract

Objectives: Our previous *in vitro* study showed that 5-(3, 4, 5-trimethoxybenzoyl)-4-methyl-2-(p-tolyl) imidazol (BZML) is a novel colchicine binding site inhibitor with potent anti-cancer activity against apoptosis resistance in A549/Taxol cells through mitotic catastrophe (MC). However, the mechanisms underlying apoptosis resistance in A549/Taxol cells remain unknown. To clarify these mechanisms, in the present study, we investigated the molecular mechanisms of apoptosis and autophagy, which are closely associated with MC in BZML-treated A549 and A549/Taxol cells.

Methods: Xenograft NSCLC models induced by A549 and A549/Taxol cells were used to evaluate the efficacy of BZML *in vivo*. The activation of the mitochondrial apoptotic pathway was assessed using JC-1 staining, Annexin V-FITC/PI double-staining, a caspase-9 fluorescence metric assay kit and western blot. The different functional forms of autophagy were distinguished by determining the impact of autophagy inhibition on drug sensitivity.

Results: Our data showed that BZML also exhibited desirable anti-cancer activity against drug-resistant NSCLC *in vivo*. Moreover, BZML caused ROS generation and MMP loss followed by the release of cytochrome c from mitochondria to cytosol in both A549 and A549/Taxol cells. However, the ROS-mediated apoptotic pathway involving the mitochondria that is induced by BZML was only fully activated in A549 cells but not in A549/Taxol cells. Importantly, we found that autophagy acted as a non-protective type of autophagy during BZML-induced apoptosis in A549 cells, whereas it acted as a type of cytoprotective autophagy against BZML-induced MC in A549/Taxol cells.

Conclusions: Our data suggest that the anti-apoptosis property of A549/Taxol cells originates from a defect in activation of the mitochondrial apoptotic pathway, and autophagy inhibitors can potentiate BZML-induced MC to overcome resistance to mitochondrial apoptosis.

1 | INTRODUCTION

Non-small-cell lung cancer (NSCLC), which is frequently unresectable, accounts for more than 80% of all lung cancers. The current available therapies include chemotherapy, molecularly targeted therapy, radiotherapy and immunotherapy.[1-4] Among them, chemotherapy has been the mainstay of treatment for decades.[5] However, chemo-resistance is also frequently encountered in the failure of NSCLC treatment.

Traditionally, the main mode of action of chemotherapeutic drugs is the induction of programmed cell death (PCD), including apoptosis and autophagy.[6-10] Apoptosis is a major mechanism that eliminates cancer cells through multiple signalling pathways. Cellular redox reactions play a major role in apoptosis. Excessive reactive oxygen species (ROS) can induce the disruption of the mitochondrial membrane potential (MMP) and the release of cytochrome c from mitochondria to cytoplasm, and can trigger caspase-dependent mitochondrial apoptosis.[11,12] In contrary, GSH, an ROS scavenger, plays a protective role against oxidative agents and leads to apoptosis resistance in cancer cells by eliminating intracellular ROS.[13,14] Additionally, GSH-based detoxification also causes apoptosis resistance in numerous cancer cells.[15-17] Thus, excessive ROS production along with GSH depletion can effectively enhance anti-cancer drug activity and overcome drug resistance.[18-20]

Apoptosis has been a prevalent model in anti-cancer drug development, but de-regulated apoptotic signalling often leads to an increase of apoptosis resistance in cancer cells with the progression of treatment.[21,22] Additionally, autophagy has been proposed as a tumour suppressor, plays a key pro-survival role in cells by eliminating damaged organelles and proteins, and contributes apoptosis resistance in cancer cells.[23-26] Importantly, the different functional forms of autophagy depend on the genetic background of cells, the microenvironment and the type of drug.[27,28] Recently, other types of PCD, including necroptosis, MC and senescence, have been reported.[10,29-31] MC, a p53-independent apoptosis-like cell death mode to against apoptosis resistance, has received more attention.[10,30] Generally, drugs cannot fully kill cancer cells by only one type of PCD and, therefore, may easily induce multidrug resistance (MDR).[23,30] Therefore, developing novel anti-cancer drugs with multiple PCD models is necessary.

Our previous study has shown that 5-(3, 4, 5-trimethoxybenzoyl) -4-methyl-2-(p-tolyl) imidazol (BZML), a novel colchicine-binding site inhibitor, has broad-spectrum anti-cancer activity against various chemo-sensitive or resistant cancer cells *in vitro*.[10] Importantly, BZML can force cells to die through apoptosis in A549 cells, whereas it mainly drives A549/Taxol cells to die by MC to against apoptosis resistance.[10] However, the apoptosis-resistant mechanisms in A549/Taxol cells have not been fully understood. In the present study, we elucidate the mechanisms underlying the apoptosis resistance in BZML-treated A549/Taxol cells, which will provide a new reference for using BZML as an anti-cancer drug to overcome drug-resistant NSCLC.

2 | MATERIALS AND METHODS

2.1 | Chemical compounds and reagents

BZML was synthesized by our group (the purity ≥98%). Paclitaxel injection was purchased from Cisen Pharmaceutical Co., Ltd (Shandong, P.C.R.). Propidium iodide (PI), monodansylcadaverine (MDC), arcidine organe (AO) and chloroquine (CQ) were purchased from Sigma Chemical (St. Louis, MO, USA). 3-methyladenine (3-MA) and rapamycin (Rapa) were purchased from Selleck Chemicals (Houston, TX, USA). Hoechst 33342, N-acetyl-L-cysteine (NAC), 2',7'-dichlorofluorescein (DCFH-DA), GSH and GSSG assay Kit, 5,5',6,6'-tetrachloro-1,1',3,3'-tetraethyl-imidacarbocyanine iodide (JC-1) and Mitochondrial Isolation Kit were from Beyotime (Nanjing, P.R.C.). Annexin V-FITC/PI double-staining kit and the caspase-9 fluorescence metric assay kit were from KeyGen (Nanjing, P.R.C.). Z-LEHD-FMK was obtained from R&D Systems, Inc. (Minneapolis, MN, USA). All antibodies were obtained from Proteintech Group (Chicago, IL, USA).

2.2 | Cell culture

A549 and A549/Taxol cells were grown in RPMI 1640 supplemented with 10% FBS at 37°C with 5% CO_2 in a humidified incubator. A549/Taxol cells were periodically cultured in 300 nM Taxol to maintain MDR and shifted into Taxol-free medium for 1 week before used.[10]

2.3 | Antitumour effects *in vivo*

All animal studies were performed in accordance with the guidelines of the Animal Experimental Ethics Committee of Shenyang Pharmaceutical University. Xenograft tumours were generated in 5-week-old male BALB/c nude mice (Huafukang Bioscience Co. Inc., Beijing, P.R.C.) using A549 or A549/Taxol cells (5×10^6 cells/mice). The tumour volumes were calculated by digital calliper measurement using the following formula: (length × width^2)/2. When the tumour volumes reached 100 mm^3, mice were randomized into 3 groups that received the following: model (vehicle, 5% ethanol+20% PEG-400+75% saline), Taxol (10 mg/kg, Taxol injection diluted in saline) and BZML (10 mg/kg, dissolved in the same vehicle as the model group). Mice were intraperitoneally administered these drugs every 3 days. By the end of the experiment, all tumours and organs were collected and measured.

2.4 | Immunohistochemistry assay

The embedded tumour tissue sections were deparaffinated, hydrated and stained with immunohistochemistry for PCNA as previously described.[9]

2.5 | ROS measurement

DCFH-DA was used for intercellular ROS measurement. Cells were treated with BZML for the indicated time periods, further incubated with DCFH-DA for 15 minutes at 37°C in the dark and then analysed by FACS (Becton-Dickinson, Frabklin Lakes, NJ, USA).

2.6 | Determination of proliferation inhibitory effect and apoptosis

The proliferation inhibitory effect of BZML was determined by MTT assay as described previously.[7] The apoptosis-like cells were

detected by Annexin V-FITC/PI double-staining and analysed by FACS as described previously.[7]

2.7 | Cell morphology changes

The cells were incubated with BZML for 36 hours and photographed using a fluorescence microscope (Olympus, Japan) after Hoechst 33342 staining.

2.8 | Cell cycle analysis

Cell cycle was detected by 70% (v/v) ethanol fixing and PI staining as described previously.[10] The samples were analysed by FACS.

2.9 | MMP assay

Cells were treated with BZML for indicated time followed by JC-1 staining for 30 minutes at 37°C in the dark. Next, samples were analysed by a fluorescence microscope or FACS.

2.10 | Preparation of cytoplasmic and mitochondrial fractions

After BZML treatment for indicated time, the cytoplasm and mitochondria were isolated using Mitochondrial Isolation Kit according to the manufacturer's instructions.

2.11 | Caspase-9 activity

Drug-stimulated activity of caspase-9 was measured using the caspase-9 fluorescence metric assay kit according to the manufacturer's instructions. The caspase-9 activity was calculated by the fold of the fluorescence intensity of BZML-treated group to that of control.

2.12 | Measurement of GSH and GSSG

Cells were treated with BZML for indicated time. The total GSH and GSSG levels were determined by GSH and GSSG Assay Kit. All steps in the procedure were based on the manufacturer's instructions.

2.13 | Immunofluorescence staining

Immunofluorescence analysis was performed as previously described and photographed by confocal microscopy (Nikon C2, Japan).[7]

2.14 | Detection of AVOs and autophagic vacuoles

To detect acidic vesicular organelles (AVOs), cells were labelled with AO and visualized by a fluorescence microscope. Autophagic vacuoles were detected with MDC and detected by FACS or a fluorescence microscope.

2.15 | Western blot analysis

Western blot was performed as described previously.[8] Densitometry analysis was done using Image J2 software.

2.16 | Statistical analysis

Data are expressed as mean ± SD of three experiments and were assessed through one-way analysis of variance by SPSS 22.0 software. $P < .05$ was considered as statistical significance.

3 | RESULTS

3.1 | BZML inhibits the growth of Taxol-sensitive and Taxol-resistant human tumour xenografts *in vivo*

In this study, A549 cell-bearing mice with BZML or Taxol treatment showed attenuated tumour growth when compared with mice in the model group (Figure 1A). The overall size and weight of tumours in the BZML- or Taxol-treated groups were significantly lower than those in the model group. As expected, there was no significant difference in the tumour size and weights between the Taxol and model groups in A549/Taxol cell-bearing mice, indicating that the tumour xenografts in A549/Taxol cell-bearing mice are resistant to Taxol. However, both the tumour growth and tumour volumes/weights were significantly reduced by BZML in A549/Taxol cell-bearing mice (Figure 1A-C).

The slightly decreased body weights in BZML-treated mice could be recovered with the extension of treatment time. Importantly, according to the viscera index analysis (the ratio of visceral weight to body weight [mg/g]), no differences were observed in the heart, liver, lung and kidney of the mice between the BZML and model groups, suggesting that this compound has low toxicity (Figure 1E).

PCNA is a nucleoprotein that localizes to eukaryotic cell nuclei and acts as a proliferative marker.[32,33] As shown in Figure 1F, high rates of PCNA-positive cells were observed in the model group. Taxol inhibited the rate of PCNA-positive cells in the tumours of A549 but not A549/Taxol cell-bearing mice. Instead, after treatment with BZML, there was a significant decrease in the rates of PCNA-positive cells in tumours of both of these two mice models.

3.2 | BZML-induced cell death is dependent on ROS in A549 cells but not in A549/Taxol cells

ROS is well-known to play an important role in inducing cell death.[8] Here, ROS was induced in a time-dependent manner in both BZML-treated A549 and A549/Taxol cells (Figure 2A). Meanwhile, BZML-induced ROS production was reversed by NAC, an effective ROS scavenger (Figure 2B).

Further, BZML-treated A549 and A549/Taxol cells in the presence or absence of NAC for 72 hours were detected by Annexin

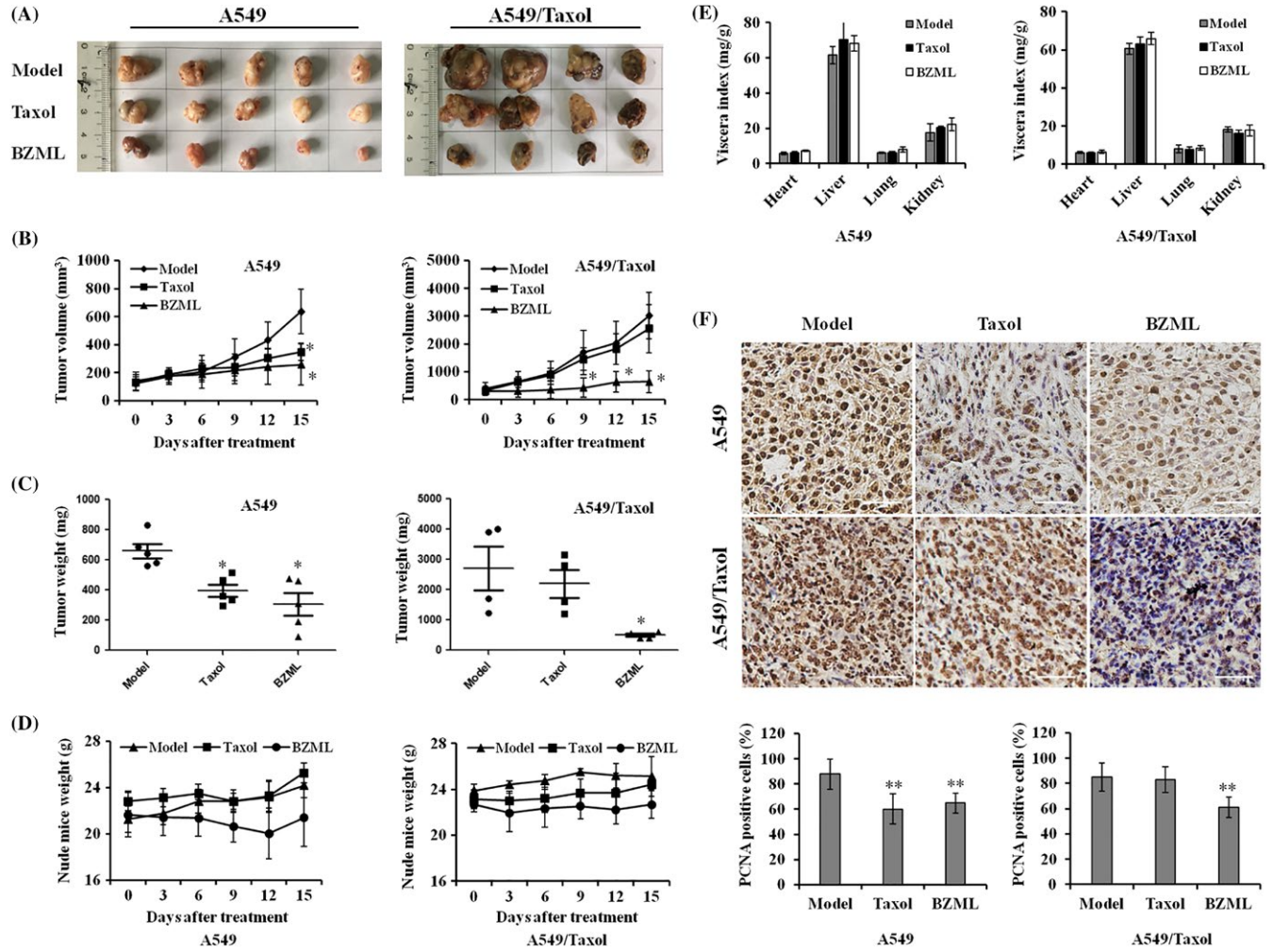

FIGURE 1 Anti-cancer effects of BZML *in vivo*. (A) Images of resected xenograft samples. (B) Average tumour volumes. (C) Average tumour weight. (D) The body weights of mice. (E) The viscera indexes of mice main organs. (F) Immunohistochemical staining of PCNA in tumour tissues (Scale bar = 100 μm); quantification (down). **P* < .05, ***P* < .01 vs the model group

V-FITC/PI staining and the MTT assay. However, the phosphatidylserine in outer cell membrane (Annexin V-FITC positive) is a marker of apoptosis, and BZML-induced MC also possesses this feature in A549/Taxol cells.[10] Here, the BZML-induced Annexin V-FITC-positive cells were clearly reduced by NAC in A549 cells, but not in A549/Taxol cells (Figure 2C). Similarly, pretreatment with NAC also did not affect the proliferation inhibitory effect of BZML in A549/Taxol cells (Figure 2D). MC acts as an apoptosis-like death mode that differs from apoptosis with unique nuclear alterations, such as multi- and/or micro-nucleation.[10] Examination of cell morphology (Figure 2E) and the cell cycle assay (Figure 2F) showed that NAC also had no influence on the proportion of multi-nucleated cells in BZML-treated A549/Taxol cells.

3.3 | The mitochondrial apoptotic pathway is only activated in BZML-treated A549 cells but not in BZML-treated A549/Taxol cells

In many cases, mitochondrial apoptosis involves the stimulation of ROS production followed by MMP depolarization.[11,12] Upon JC-1

FIGURE 2 BZML-induced cell death is dependent on ROS in A549 cells but not in A549/Taxol cells. (A) DCFH-DA staining for ROS detection in cells treated with BZML (20 or 60 nM); quantification (right). (B) DCFH-DA staining of cells pretreated with NAC (5 mM) or vehicle for 1 hour and continually incubated with BZML (20 or 60 nM) for another 48 hours; quantification (right). (C) Annexin V-FITC/PI double-staining of cells pretreated with NAC (5 mM) or vehicle for 1 hour and continually incubated with BZML (20 or 60 nM) for another 72 hours; quantification (down). (D) MTT assay. Cells pretreated with NAC (5 mM) or vehicle for 1 hour were continually incubated with BZML (20 or 60 nM) for another 72 hours. (E) The nuclei morphology changes of A549/Taxol cells, with NAC (5 mM) or vehicle pretreatment for 1 hour and BZML (60 nM) continuous treatment for another 36 hours (scale bar = 200 μm). (F) FACS for detecting the percentage of polyploid cells with NAC (5 mM) or vehicle pretreatment for 1 hour and BZML (60 nM) continuous treatment for another 36 hours. ***P* < .01 vs control; ##*P* < .01 vs BZML-alone-treated group

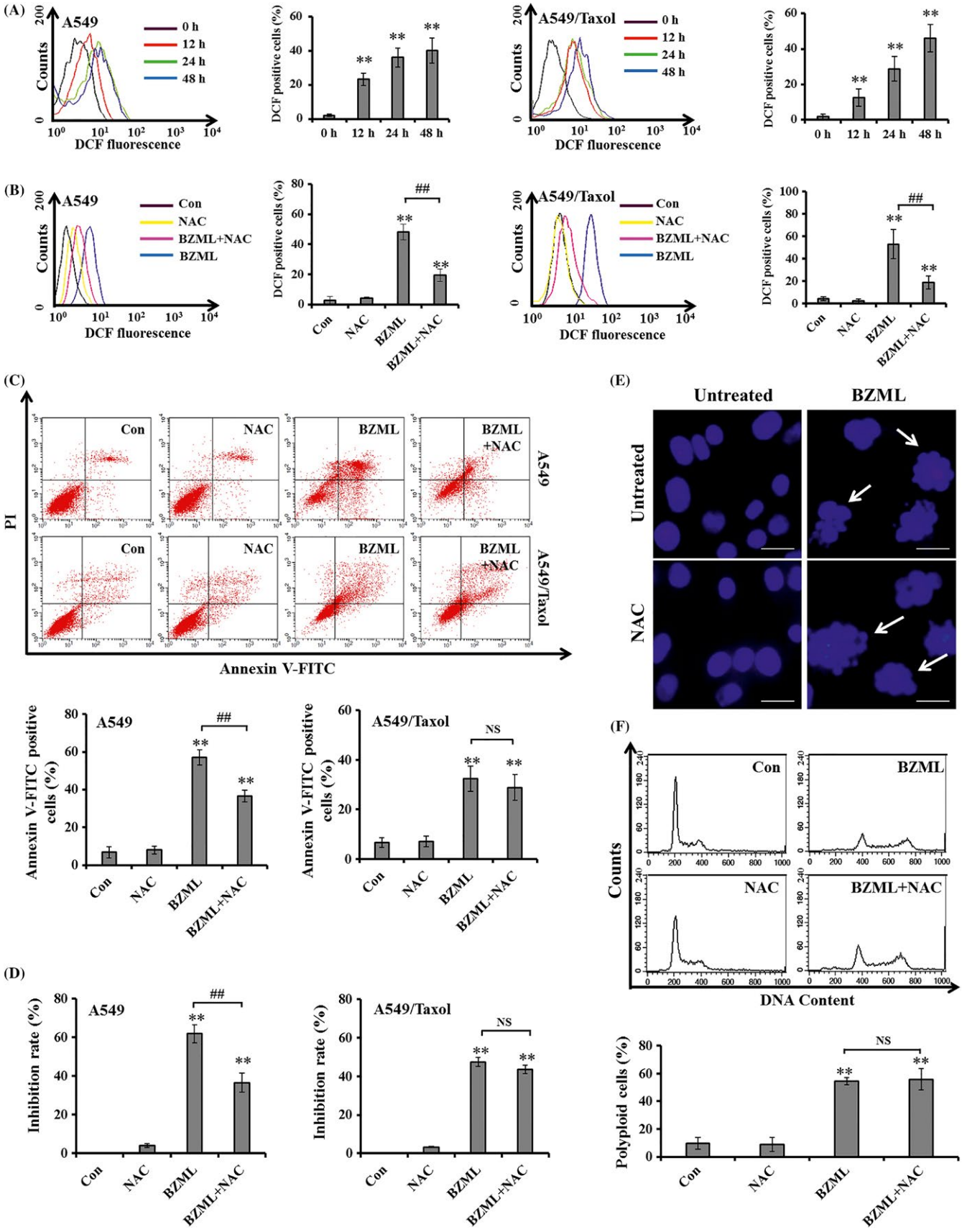

staining, the control cells showed strong red fluorescence, while BZML-treated cells exhibited enhanced green fluorescence as the incubation time increased (Figure 3A). The ratio of red to green fluorescence was measured by FACS. BZML led to an obvious decrease in the ratio in A549 and A549/Taxol cells in a time-dependent manner (Figure 3B).

The mitochondria are known to be important sites for the generation of ROS and the induction of ROS results in oxidative damage to the mitochondria.[11,12] To clarify the relationship between ROS and MMP, we inhibited ROS by NAC and determined the levels of MMP. As shown in Figure 3A,B, NAC pretreatment significantly rescued the decrease in MMP compared with the BZML-treated group. Mitochondrial damage is also associated with the release of cytochrome c from mitochondria to cytosol and activates the mitochondrial apoptotic pathway.[12] Our results showed that cytosolic cytochrome c levels increased while the mitochondrial cytochrome c levels decreased in BZML-treated A549 and A549/Taxol cells. Additionally, mitochondrial outer membrane

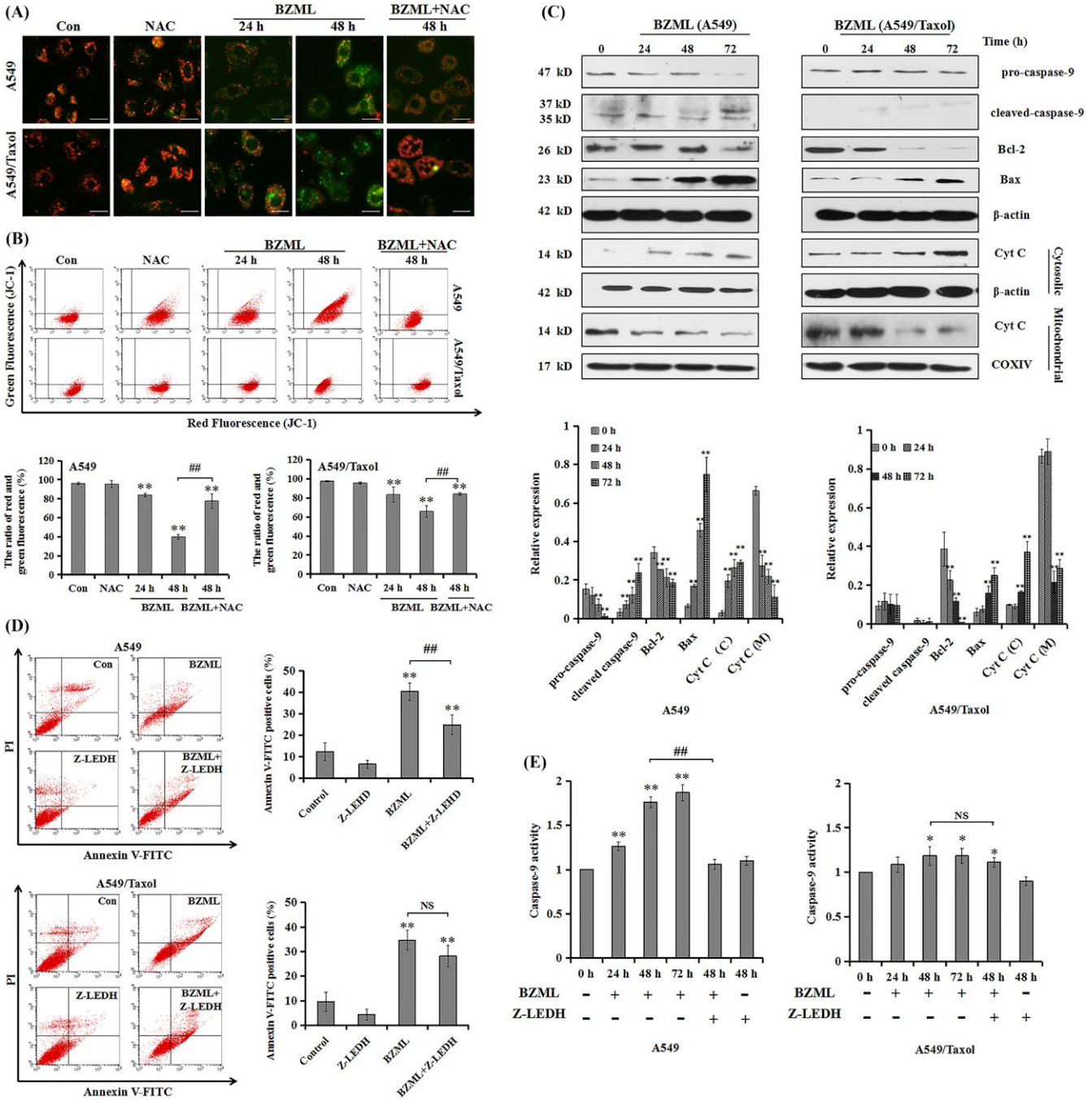

FIGURE 3 The mitochondrial apoptotic pathway is activated in BZML-treated A549 cells, but not in BZML-treated A549/Taxol cells. (A-B) JC-1 staining of cells treated with BZML (20 or 60 nM) for indicated time in the absence or presence of NAC (5 mM) was performed by fluorescence microscope and FACS, respectively. (C) Western blot showed the expression of mitochondrial apoptosis-related proteins in BZML-treated cells. (D) Annexin V-FITC/PI double staining of cells pretreated with Z-LEHD-FMK (40 μM) for 6 hours and continually incubated with BZML (20 or 60 nM) for 48 hours; quantification (right). (E) The caspase-9 activity of cells pretreated with Z-LEHD-FMK (40 μM) or vehicle for 6 hours and continually incubated with BZML (20 or 60 nM) for indicated time. $^{*}P < .05$, $^{**}P < .01$ vs control; $^{\#\#}P < .01$ vs BZML-alone-treated group

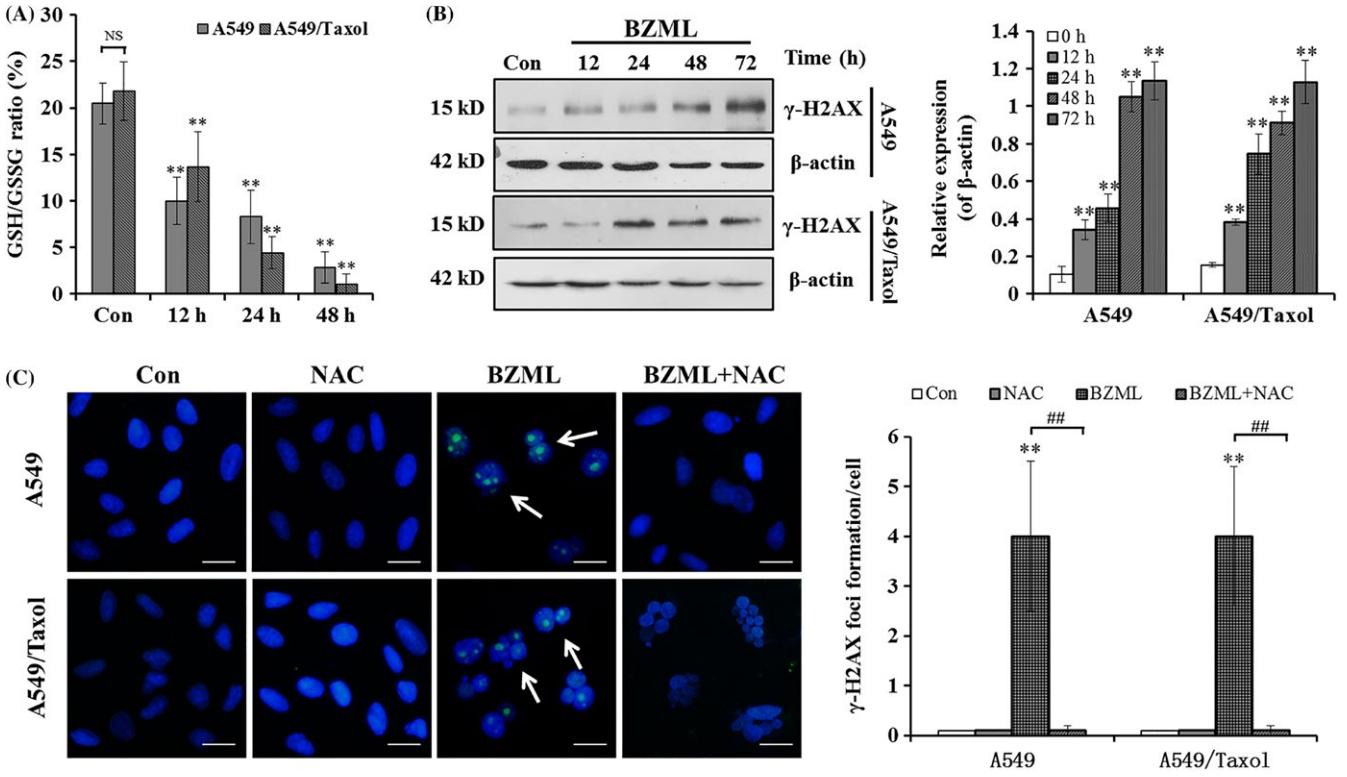

FIGURE 4 BZML causes GSH depletion and DNA damage in both A549 and A549/Taxol cells. (A) The GSH/GSSG ratio was measured at indicated time points. (B) BZML up-regulated expression of γ-H2AX protein was analysed by western blot; quantification (right). (C) Confocal microscopy analysis of the number of γ-H2AX foci formation in cells pretreated with NAC (5 mM) or vehicle for 1 hour and continually incubated with BZML (20 or 60 nM) for another 48 hours; quantification (right). The γ-H2AX foci labelled with green. Scale bar = 100 μm. $^{**}P < .01$ vs control

permeabilization can be affected by the Bcl-2 family proteins.[34,35] We found that BZML could time dependently up-regulate the expression of Bax and down-regulate the expression of Bcl-2 in A549 and A549/Taxol cells (Figure 3C). Importantly, caspase-9 acts as a mitochondrial apoptotic pathway effector.[11,12] In our study, cleaved caspase-9 was only detected in BZML-treated A549 cells (Figure 3C). Meanwhile, BZML time dependently enhanced caspase-9 activity in A549 cells, but not in A549/Taxol cells (Figure 3D). Further, the caspase-9 inhibitor Z-LEHD-FMK significantly suppressed the BZML-induced increase in caspase-9 activity and Annexin V-FITC-positive cells in A549 cells, but not in A549/Taxol cells (Figure 3D,E). All of these results suggest that BZML induces A549 cells to die through the mitochondrial apoptotic pathway, whereas BZML-treated A549/Taxol cells fail to undergo this process.

3.4 | BZML causes GSH depletion and DNA damage in both A549 and A549/Taxol cells

The GSH/GSSG ratio is widely used as an important indicator to evaluate the cellular redox system.[15-17] As shown in Figure 4A, the GSH/GSSG ratios were significantly reduced in both BZML-treated A549 and A549/Taxol cells. Interestingly, the constitutive GSH/GSSG ratios were not significantly different between A549 and A549/Taxol cells, suggesting that GSH did not contribute to apoptosis resistance in A549/Taxol cells.

Histone H2AX is known to be phosphorylated at Ser139 (γ-H2AX) immediately after DNA damage.[36,37] As shown in Figure 4B, the expression levels of γ-H2AX were increased in a time-dependent manner in both BZML-treated A549 and A549/Taxol cells. Meanwhile, pretreatment with NAC protected the BZML-treated A549 and A549/Taxol cells from the DNA damage, a finding that was reflected in the decreased number of γ-H2AX foci formation, confirming that ROS production could regulate DNA damage (Figure 4C).

3.5 | BZML induces autophagy in both A549 and A549/Taxol cells

Autophagy is often activated during chemotherapy. Here, we used MDC to assess autophagy induction *via* the accumulation of the MDC-labelled autophagosome.[6] As shown in Figure 5A, compared with the control, the percentages of MDC-positive cells were increased in a time-dependent manner in both cell lines after BZML treatment. Further, 3-MA prevented BZML-induced autophagosome formation (Figure 5B,C). Meanwhile, AVOs, an autophagy-related lysosomal structure, are monitored by labelling cells with AO.[6] Fluorescence microscopy showed a significant increase in red fluorescence after 48 hours of BZML

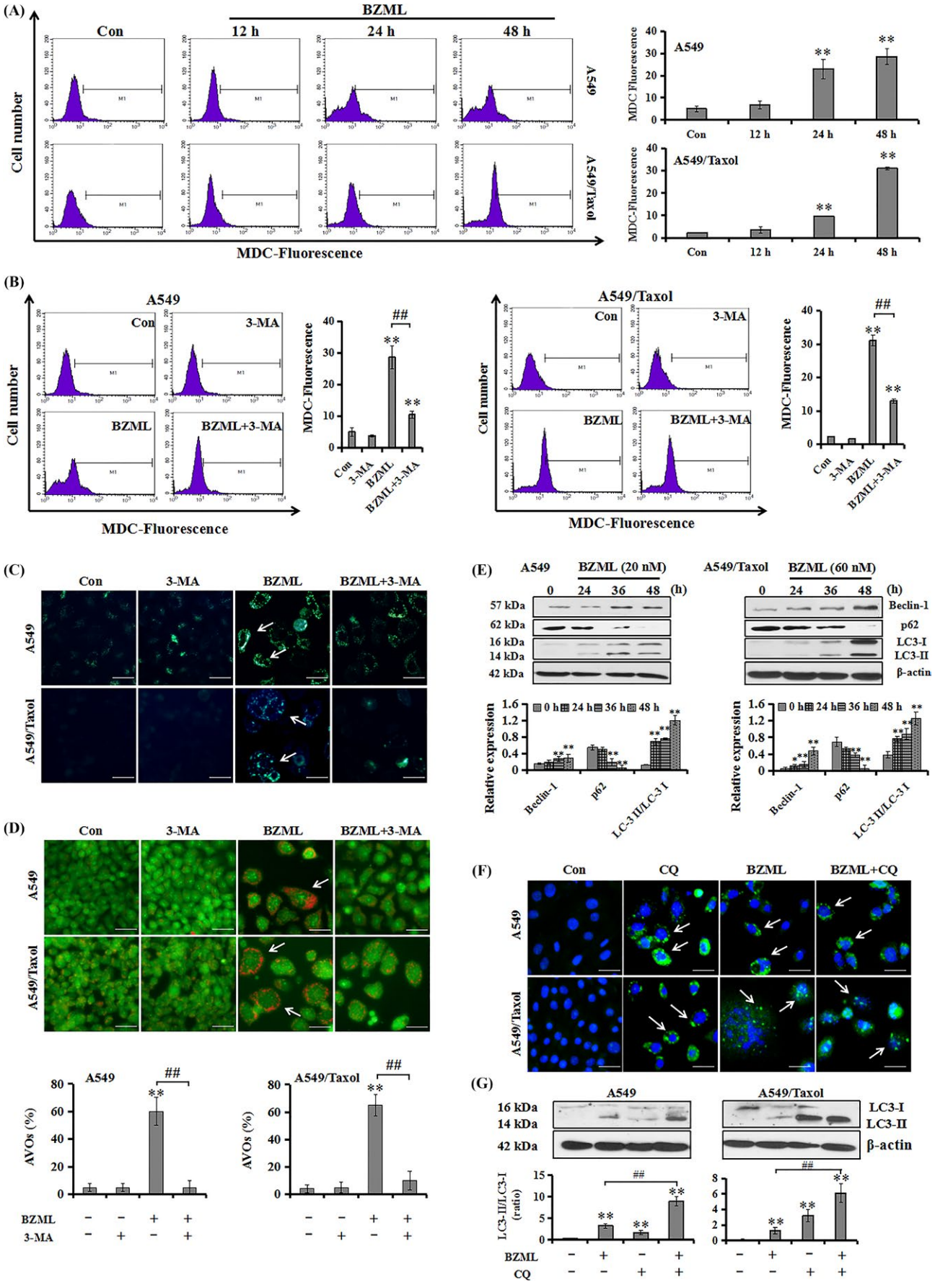
(A)
BZML
Con
12 h
24 h
48 h
A549
A549/Taxol
Cell number
MDC-Fluorescence
MDC Fluorescence
(B)
3-MA
BZML+3-MA
##
(C)
(D)
AVOs (%)
(E)
A549
A549/Taxol
BZML (20 nM)
BZML (60 nM)
57 kDa
62 kDa
16 kDa
14 kDa
42 kDa
Beclin-1
p62
LC3-I
LC3-II
β-actin
Relative expression
LC-3 II/LC-3 I
(F)
CQ
BZML+CQ
(G)
LC3-II/LC3-I (ratio)

FIGURE 5 BZML induces autophagy in both cell lines. (A-B) Cells were treated with BZML (20 or 60 nM) in the absence or presence of 3-MA (5 mM), and measured using MDC staining; quantification (right). (C) Images of MDC staining in BZML-treated cells. (D) AO staining of cells treated with BZML (20 or 60 nM) for 48 hours in the absence or presence of 3-MA (5 mM); quantification (down). (E) The expression of autophagy-related proteins in cells treated with BZML for 0-48 hours. (F) Immunofluorescence analysis of LC3 punctate formation in cells after BZML (20 or 60 nM) treatment for 48 hours in the absence or presence of CQ (2 μM) (LC3 labelled with green, nuclei with blue) (scale bar = 100 μm). (G) Western blot of LC3-II formation in cells after BZML (20 or 60 nM) treatment for 48 hours in the absence or presence of CQ (2 μM). $^{**}P < .01$ vs control; $^{\#\#}P < .01$ vs BZML-alone-treated group

incubation and was decreased by 3-MA pretreatment in both cell lines (Figure 5D).

In addition, the conversion of LC3 from LC3-I to LC3-II is a characteristic of autophagy.[24,38,39] As indicated in Figure 5E, LC3-II/LC3-I ratio was increased in A549 and A549/Taxol cells in a time-dependent manner after exposure to BZML. Moreover, BZML time dependently caused an increase in Beclin-1 and a reduction in p62 in A549 and A549/Taxol cells. Furthermore, an autophagy flux assay, which was based on the evaluation of LC3-positive autophagic puncta by confocal microscopy and LC3 conversion by western blot, showed that CQ could increase the number of fluorescent punctate autophagic vacuoles and the ratio of LC3-II to LC3-I (Figure 5F,G). Numerous punctate patterns of LC3 immunoreactivity were observed in multi-nucleated cells, suggesting that BZML-induced autophagy was associated with MC (Figure 5F).

3.6 | Autophagy plays a protective role in BZML-induced MC, but not against BZML-induced apoptosis

As autophagy is also a survival mechanism, one can speculate that autophagy induced by anti-cancer drugs might contribute to apoptosis resistance.[26] Next, we investigated the cross-talk between BZML-induced autophagy and apoptosis in A549 cells or MC in A549/Taxol cells, respectively. As shown in Figure 6A,B, 3-MA and CQ treatment had no significant effects on BZML-induced apoptosis in A549 cells, indicating that autophagy inhibition did not augment apoptosis in A549 cells. However, pretreatment with the autophagy inhibitors significantly potentiated BZML-induced apoptosis-like cell death in A549/Taxol cells, suggesting that BZML-induced MC was vulnerable to autophagy inhibition. We further examined whether autophagy inhibitors could affect the BZML-induced multi-nucleation in A549/Taxol cells. Unexpectedly, the proportion of polyploid cells was deceased, a finding that was associated with the increase in subG1 cells in A549/Taxol cells co-treated with BZML and CQ (Figure 6C).

Rapa, a classic autophagy accelerant, was used to induce autophagy.[40] As shown in Figure 6D, the number of apoptosis-like cells was markedly decreased after co-treatment with BZML and Rapa when compared with BZML treatment alone. Additionally, Rapa pretreatment prevented BZML-induced polyploid cells, which indicated that Rapa blocked the occurrence of BZML-induced MC (Figure 6E). Meanwhile, for A549/Taxol cells, BZML did not have a similar capacity to cause the increase in the proportion of polyploid cells post 24-hour BZML incubation and another 12-hour Rapa co-incubation, when compared with the BZML treatment alone for the 36-hour group (Figure 6F). Notably, Rapa treatment did not increase the number of subG1 cells in BZML-treated A549/Taxol cells (Figure 6E,F).

4 | DISCUSSION

Microtubules are important in maintaining the structure of cells and have become an excellent drug target in chemotherapy.[41-43] Currently, Taxol is widely used in the treatment of NSCLC in the clinics. However, many patients have acquired resistance to Taxol, and even those who initially respond will eventually exhibit MDR.[44-47] We have confirmed that BZML has potent anti-cancer activity against Taxol-sensitive or Taxol-resistant A549 cells through different death modes *in vitro*.[10] This paper aimed to evaluate the anti-cancer activity of BZML *in vivo* and the mechanism underlying the apoptosis resistance in BZML-treated A549/Taxol cells.

The acquired resistance in cancer cells is often associated with more malignancy, which is reflected by rapid proliferation of cancer cells and poor efficacy of anti-cancer drugs.[48,49] In our study, the therapeutic dose of Taxol used in A549 cell-bearing mice failed to inhibit tumour growth in A549/Taxol cell-bearing mice. Meanwhile, the overall size and weight of tumours in the A549/Taxol cell-bearing mice were greater than in A549 cell-bearing mice under drug-free treatment conditions, suggesting that the tumours of A549/Taxol cell-bearing mice were more malignant than those of A549 cell-bearing mice. Importantly, BZML had potent anti-cancer activity in both A549 and A549/Taxol cell-bearing mice. Additionally, the rates of PCNA-positive cells were decreased in both the BZML-treated A549 and A549/Taxol cell-bearing mice. Further, compared with the model group, the average body weight and the viscera index of mice were not significantly influenced by BZML. These results indicate that BZML exhibits potential anti-cancer effects and low toxicity on Taxol-sensitive or Taxol-resistant NSCLC *in vivo*.

Apoptosis is a major mechanism used to eliminate cancer cells, and the mitochondrial pathway plays an important role in this process.[21] In our study, BZML caused ROS generation and MMP loss followed by the release of cytochrome c from mitochondria to cytosol in A549 and A549/Taxol cells. However, activated caspase-9 was only observed in A549 cells. Moreover, the caspase-9 fluorescence metric assay showed that caspase-9 activity was increased with BZML in A549 cells, but not in A549/Taxol cells. Meanwhile, Z-LEHD-FMK, a caspase-9 inhibitor, markedly suppressed BZML-induced apoptosis in A549 cells, and this inhibitory effect was lost in A549/Taxol cells. As previous reports, BZML-treated A549/

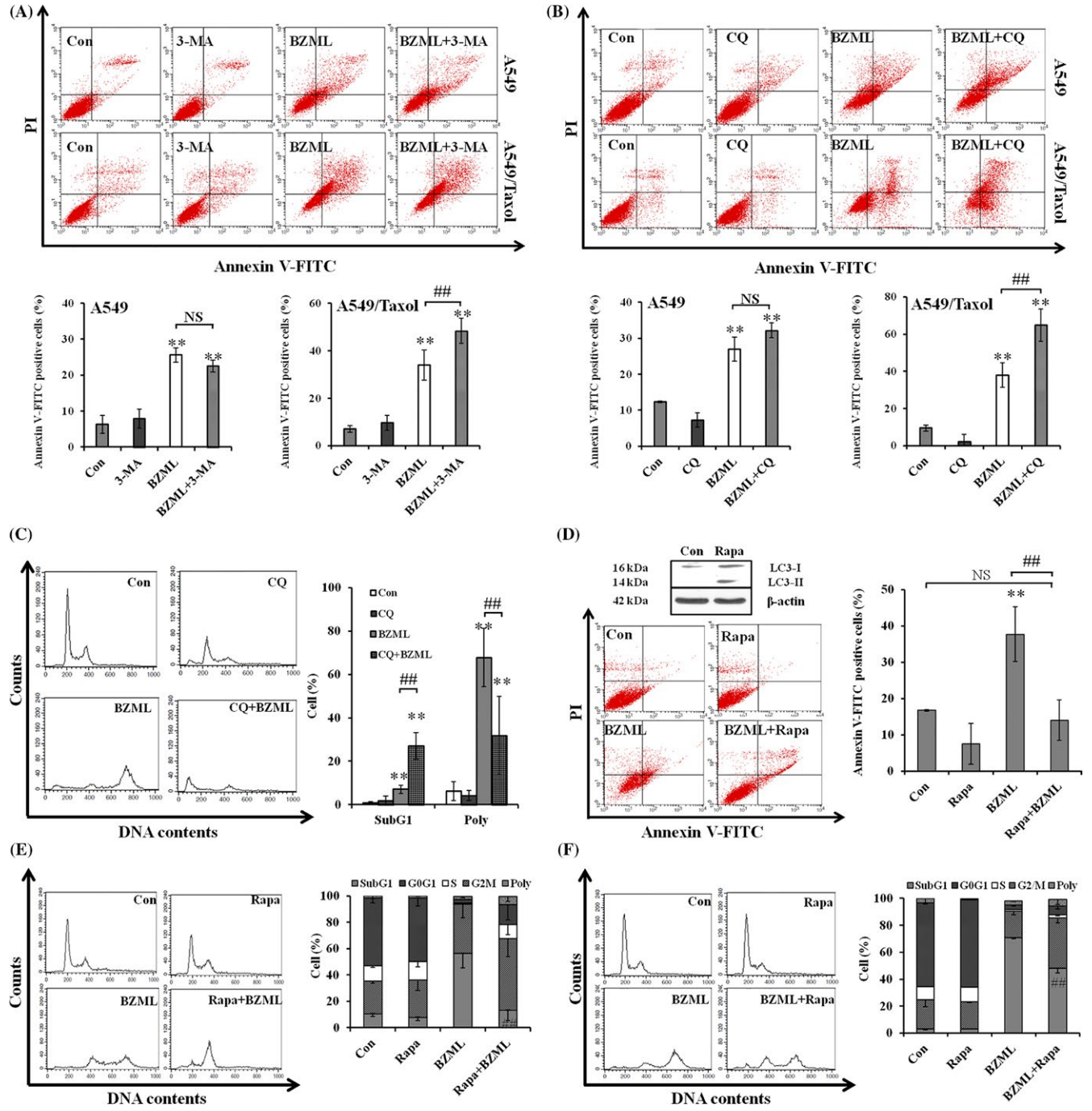

FIGURE 6 Autophagy plays a protective role in BZML-induced MC, but not against BZML-induced apoptosis. (A) Annexin V-FITC/PI double-staining of cells pretreated with 3-MA (5 mM) or vehicle for 2 hours and continually incubated with BZML (20 or 60 nM) for another 48 hours; quantification (down). (B) Annexin V-FITC/PI double staining of cells pretreated with CQ (2 μM) or vehicle for 2 hours and continually incubated with BZML (20 or 60 nM) for another 48 hours; quantification (down). (C) FACS analysis for cell cycle distribution after pretreatment with CQ (2 μM) or vehicle for 2 hours, followed by BZML (60 nM) treatment for another 36 hours in A549/Taxol cells. (D) Annexin V-FITC/PI double staining for apoptosis-like cells measurement in A549/Taxol cells pretreated with Rapa (20 nM) or vehicle for 2 hours and continually incubated with BZML (60 nM) for another 48 hours. (E) FACS analysis for A549/Taxol cell cycle distribution after pretreatment with Rapa (20 nM) or vehicle for 2 hours, followed by BZML (60 nM) treatment for another 36 hours. (F) FACS analysis for the percentage of cells in specific cell cycle phase. A549/Taxol cells were pre-incubated with BZML for 24 hours and followed by another 12-hour co-incubation with Rapa (20 nM). $^{**}P < .01$ vs control; $^{\#\#}P < .01$ vs BZML-alone-treated group

Taxol cells might have anti-apoptosis properties.[10] In this study, we demonstrated that BZML could induce A549 cell apoptosis through mitochondrial apoptotic pathway, a feature that was not seen in BZML-treated A549/Taxol cells. Therefore, the anti-apoptosis properties of A549/Taxol cells might result from the defect in activation of the mitochondrial apoptotic pathway.

Furthermore, oxidative stress mediated by ROS is a key mechanism for mitochondrial apoptosis stimulated by anti-cancer drugs. BZML can induce ROS production in both A549 and A549/Taxol cells. However, ROS had no influence on the proportion of multinucleated cells in BZML-treated A549/Taxol cells. Meanwhile, GSH acts as a free radical scavenger and plays a protective role against ROS-mediated anti-cancer effects.[15-17] Importantly, the overexpression of GSH has been associated with chemo- and radio-resistance in cancer cells.[13,14] Therefore, GSH depletion is considered to be an effective strategy to sensitize cancer cells to therapy. Here, ROS did not play a role in inducing cell death, and GSH did not contribute to the resistance to mitochondrial apoptosis in A549/Taxol cells; however, ROS generation could still damage DNA and other cellular components to destroy cellular functions and lead to GSH depletion, which, in part, blocked the occurrence of apoptosis resistance mediated by GSH.

Most studies have reported that autophagy is an important factor for apoptosis resistance.[26,39] Thus, our study mainly focused on clarifying the interaction between autophagy and MC. Currently, four different functional forms of autophagy, including cytoprotective (cell survival), cytotoxic (cell death), non-protective (no contribution to cell death and survival) and cytostatic (growth arrest) autophagy, have been proposed to be induced during chemotherapy.[50-52] The different functional forms of autophagy are almost exclusively distinguished by determining the impact of autophagy inhibition on drug sensitivity.[50,51] In our study, different functional forms of autophagy were activated during different death modes caused by BZML in A549 and A549/Taxol cells, respectively. Autophagy inhibitors have no impact on BZML-treated A549 cells, suggesting that autophagy acts as a type of non-protective autophagy during BZML-induced apoptosis in A549 cells. In contrast, cytoprotective autophagy was only detected in BZML-induced MC through CQ and 3-MA increasing the number of apoptosis-like cells in A549/Taxol cells. Further, Rapa reduced the number of BZML-induced apoptosis-like cells in A549/Taxol cells. Surprisingly, CQ did not increase the proportion of polyploid cells to sensitize the anti-cancer activity of BZML but rather increased the population of subG1 cells accompanied by a decrease in polyploid cells in BZML-treated A549/Taxol cells. Interestingly, the proportion of polyploid cells was decreased by Rapa with post-treatment or pretreatment with BZML in A549/Taxol cells. Meanwhile, pretreatment with Rapa also did not cause MC occurrence in BZML-treated A549 cells (data not shown). Additionally, some studies have found that MC occurrence is independent of autophagy.[53,54] Therefore, these findings suggest that autophagy can block the occurrence and development of MC but cannot contribute to resistance to mitochondrial apoptosis to induce MC in BZML-treated A549/Taxol cells. In other words, our data proved that autophagy is only required for cell survival under BZML-induced MC in A549/Taxol cells. Interestingly, MC acts as a novel death mode against resistance to mitochondrial apoptosis and requires a relatively longer time to drive a cell to die in classical apoptosis.[30,55-57] The final outcome of MC is also cell death, but the longer death process is not beneficial for chemotherapy. Therefore, we speculate that autophagy played a cytoprotective role against BZML-induced MC in A549/Taxol cells, and the inhibition of autophagy can accelerate the death of BZML-induced MC cells. Furthermore, this assumption may be used to explain the longer duration of cell death in BZML-induced MC cells. However, the exact mechanisms underlying the different functional forms of autophagy induced by BZML still require further investigation and may correlate with the genetic background of cells.

In conclusion, BZML also exerts potent anti-cancer activity against Taxol-sensitive and Taxol-resistant NSCLC *in vivo*. BZML activates the ROS-mediated mitochondrial apoptotic pathway in A549 cells, while this pathway cannot be fully activated by BZML in A549/Taxol cells. These findings indicate that the anti-apoptosis properties of A549/Taxol cells may originate from a defect in activation of the mitochondrial apoptotic pathway. The inactivation of the death mode mediated by mitochondrial apoptosis is replaced by MC, which ultimately forces BZML-treated A549/Taxol cells to die. Importantly, autophagy acts as a type of non-protective autophagy during BZML-induced apoptosis in A549 cells, whereas it acts as a type of cytoprotective autophagy and contributes to the longer duration of cell death against BZML-induced MC in A549/Taxol cells. Hence, our studies provide further insight into the anti-cancer mechanism of BZML. The excellent anti-cancer activity of BZML is worthy of further preclinical research for a promising anti-cancer drug, and autophagy inhibition could potentiate BZML-induced MC to overcome the resistance to mitochondrial apoptosis. These findings may provide a novel therapeutic approach against drug-resistant NSCLC.

ACKNOWLEDGEMENTS

This work was supported by grants from the National Natural Science Foundation (8160130989 and 8167130571), Education Foundation of Liaoning Province (201610163L12), Doctoral Scientific Research Foundation of Liaoning Province (201601144) and Young and middle age backbone personnel training programme of Shenyang Pharmaceutical University (ZQN2015003).

CONFLICT OF INTEREST

The authors declare no conflict of interest.

ORCID

Yingliang Wu http://orcid.org/0000-0002-5155-7568

REFERENCES

1. Chen W, Zheng R, Baade PD, et al. Cancer statistics in China, 2015. *CA Cancer J Clin*. 2016;66:115-132.

2. Siegel RL, Miller KD, Jemal A. Cancer statistics, 2016. *CA Cancer J Clin*. 2016;66:7-30.
3. Cho JH. Immunotherapy for non-small-cell lung cancer: current status and future obstacles. *Immune Netw*. 2017;17:378-391.
4. Malhotra J, Jabbour SK, Aisner J. Current state of immunotherapy for non-small cell lung cancer. *Transl Lung Cancer Res*. 2017;6:196-211.
5. Miller KD, Siegel RL, Lin CC, et al. Cancer treatment and survivorship statistics, 2016. *CA Cancer J Clin*. 2016;66:271-289.
6. Viola G, Bortolozzi R, Hamel E, et al. MG-2477, a new tubulin inhibitor, induces autophagy through inhibition of the Akt/mTOR pathway and delayed apoptosis in A549 cells. *Biochem Pharmacol*. 2012;83:16-26.
7. Qi H, Zuo DY, Bai ZS, et al. COH-203, a novel microtubule inhibitor, exhibits potent anti-tumor activity via p53-dependent senescence in hepatocellular carcinoma. *Biochem Biophys Res Commun*. 2014;455:262-268.
8. Xu J, Zuo D, Qi H, et al. 2-Methoxy-5((3,4,5-trimethosyphenyl)seleninyl) phenol (SQ0814061), a novel microtubule inhibitor, evokes G2/M cell cycle arrest and apoptosis in human breast cancer cells. *Biomed Pharmacother*. 2016;78:308-321.
9. Xu J, Han M, Shen J, et al. 2-Methoxy-5((3,4,5-trimethosyphenyl) seleninyl) phenol inhibits MDM2 and induces apoptosis in breast cancer cells through a p53-independent pathway. *Cancer Lett*. 2016;383:9-17.
10. Bai Z, Gao M, Zhang H, et al. BZML, a novel colchicine binding site inhibitor, overcomes multidrug resistance in A549/Taxol cells by inhibiting P-gp function and inducing mitotic catastrophe. *Cancer Lett*. 2017;402:81-92.
11. Mukhopadhyay S, Das DN, Panda PK, et al. Autophagy protein Ulk1 promotes mitochondrial apoptosis through reactive oxygen species. *Free Radic Biol Med*. 2015;89:311-321.
12. Wen C, Chen J, Zhang D, et al. Pseudolaric acid B induces mitotic arrest and apoptosis in both 5-fluorouracil-sensitive and -resistant colorectal cancer cells. *Cancer Lett*. 2016;383:295-308.
13. Jozefczak M, Remans T, Vangronsveld J, et al. Glutathione is a key player in metal-induced oxidative stress defenses. *Int J Mol Sci*. 2012;13:3145-3175.
14. Traverso N, Ricciarelli R, Nitti M, et al. Role of glutathione in cancer progression and chemoresistance. *Oxid Med Cell Longev*. 2013;2013:972913.
15. Li Q, Zhan M, Chen W, et al. Phenylethyl isothiocyanate reverses cisplatin resistance in biliary tract cancer cells via glutathionylation-dependent degradation of Mcl-1. *Oncotarget*. 2016;7:10271-10282.
16. Rocha CR, Kajitani GS, Quinet A, et al. NRF2 and glutathione are key resistance mediators to temozolomide in glioma and melanoma cells. *Oncotarget*. 2016;7:48081-48092.
17. Meng L, Xia X, Yang Y, et al. Co-encapsulation of paclitaxel and baicalein in nanoemulsions to overcome multidrug resistance via oxidative stress augmentation and P-glycoprotein inhibition. *Int J Pharm*. 2016;513:8-16.
18. Lorendeau D, Dury L, Genoux-Bastide E, et al. Collateral sensitivity of resistant MRP1-overexpressing cells to flavonoids and derivatives through GSH efflux. *Biochem Pharmacol*. 2014;90:235-245.
19. Sun W, Bao J, Lin W, et al. 2-Methoxy-6-acetyl-7-methyljuglone (MAM), a natural naphthoquinone, induces NO-dependent apoptosis and necroptosis by H2O2-dependent JNK activation in cancer cells. *Free Radic Biol Med*. 2016;92:61-77.
20. Drozd E, Krzyszton-Russjan J, Marczewska J, et al. Up-regulation of glutathione-related genes, enzyme activities and transport proteins in human cervical cancer cells treated with doxorubicin. *Biomed Pharmacother*. 2016;83:397-406.
21. Vitale I, Galluzzi L, Castedo M, et al. Mitotic catastrophe: a mechanism for avoiding genomic instability. *Nat Rev Mol Cell Biol*. 2011;12:385-392.
22. Mohammad RM, Muqbil I, Lowe L, et al. Broad targeting of resistance to apoptosis in cancer. *Semin Cancer Biol*. 2015;35(Suppl):S78-S103.
23. Zhang C, Yang L, Wang XB, et al. Calyxin Y induces hydrogen peroxide-dependent autophagy and apoptosis via JNK activation in human non-small cell lung cancer NCI-H460 cells. *Cancer Lett*. 2013;340:51-62.
24. Lee SY, Oh JS, Rho JH, et al. Retinal pigment epithelial cells undergoing mitotic catastrophe are vulnerable to autophagy inhibition. *Cell Death Dis*. 2014;5:e1303.
25. Sharma K, Goehe RW, Di X, et al. A novel cytostatic form of autophagy in sensitization of non-small cell lung cancer cells to radiation by vitamin D and the vitamin D analog, EB 1089. *Autophagy*. 2014;10:2346-2361.
26. Jing Z, Sui X, Yao J, et al. SKF-96365 activates cytoprotective autophagy to delay apoptosis in colorectal cancer cells through inhibition of the calcium/CaMKIIgamma/AKT-mediated pathway. *Cancer Lett*. 2016;372:226-238.
27. Hale AN, Ledbetter DJ, Gawriluk TR, et al. Autophagy: regulation and role in development. *Autophagy*. 2013;9:951-972.
28. Tan YQ, Zhang J, Zhou G. Autophagy and its implication in human oral diseases. *Autophagy*. 2017;13:225-236.
29. Castedo M, Perfettini JL, Roumier T, et al. Mitotic catastrophe constitutes a special case of apoptosis whose suppression entails aneuploidy. *Oncogene*. 2004;23:4362-4370.
30. Denisenko TV, Sorokina IV, Gogvadze V, et al. Mitotic catastrophe and cancer drug resistance: a link that must to be broken. *Drug Resist Updat*. 2016;24:1-12.
31. Llovera L, Mansilla S, Portugal J. Apoptotic-like death occurs through a caspase-independent route in colon carcinoma cells undergoing mitotic catastrophe. *Cancer Lett*. 2012;326:114-121.
32. Zhang W, Lan Y, Huang Q, et al. Galangin induces B16F10 melanoma cell apoptosis via mitochondrial pathway and sustained activation of p38 MAPK. *Cytotechnology*. 2013;65:447-455.
33. Kumar R, Herold JL, Schady D, et al. Streptococcus gallolyticus subsp. gallolyticus promotes colorectal tumor development. *PLoS Pathog*. 2017;13:e1006440.
34. Reyna DE, Garner TP, Lopez A, et al. Direct Activation of BAX by BTSA1 overcomes apoptosis resistance in acute myeloid leukemia. *Cancer Cell*. 2017;32:490-505.
35. Birkinshaw RW, Czabotar PE. The BCL-2 family of proteins and mitochondrial outer membrane permeabilisation. *Semin Cell Dev Biol*. 2017;72:152-162.
36. Wang YY, Chen YK, Hu SC, et al. CYT-Rx20 inhibits ovarian cancer cells in vitro and in vivo through oxidative stress-induced DNA damage and cell apoptosis. *Cancer Chemother Pharmacol*. 2017;79:1129-1140.
37. Ruiz-Magana MJ, Martinez-Aguilar R, Lucendo E, et al. The antihypertensive drug hydralazine activates the intrinsic pathway of apoptosis and causes DNA damage in leukemic T cells. *Oncotarget*. 2016;7:21875-21886.
38. Wang M, Liao C, Hu Y, et al. Sensitization of breast cancer cells to paclitaxel by dichloroacetate through inhibiting autophagy. *Biochem Biophys Res Commun*. 2017;489:103-108.
39. Jiang XS, Chen XM, Wan JM, et al. Autophagy protects against palmitic acid-induced apoptosis in podocytes in vitro. *Sci Rep*. 2017;7:42764.
40. Lee SY, Oh JS, Rho JH, et al. *Rapamycin regulates autophagy and cell adhesion in induced pluripotent stem cells*. 2016;7:166.
41. Parker AL, Teo WS, McCarroll JA, et al. An emerging role for tubulin isotypes in modulating cancer biology and chemotherapy resistance. *Int J Mol Sci*. 2017;18:1434.
42. Arnst KE, Wang Y, Hwang DJ, et al. A potent, metabolically stable tubulin inhibitor targets the colchicine binding site and overcomes taxane resistance. *Cancer Res*. 2018;78:265-277.

43. Mills CC, Kolb EA, Sampson VB. Recent advances of cell-cycle inhibitor therapies for pediatric cancer. *Cancer Res*. 2017;77:6489-6498.
44. El-Araby ME, Omar AM, Khayat MT, et al. Molecular mimics of classic P-glycoprotein inhibitors as multidrug resistance suppressors and their synergistic effect on paclitaxel. *PLoS ONE*. 2017;12:e0168938.
45. Datta S, Choudhury D, Das A, et al. Paclitaxel resistance development is associated with biphasic changes in reactive oxygen species, mitochondrial membrane potential and autophagy with elevated energy production capacity in lung cancer cells: a chronological study. *Tumour Biol*. 2017;39:1010428317694314.
46. Shi X, Dou Y, Zhou K, et al. Targeting the Bcl-2 family and P-glycoprotein reverses paclitaxel resistance in human esophageal carcinoma cell line. *Biomed Pharmacother*. 2017;90:897-905.
47. Wu GX, Nelson RA, Kim JY, et al. Non-small cell lung cancer as a second primary among patients with previous malignancy: who is at risk. *Clin Lung Cancer*. 2017;18:543-550.
48. Zhang W, Shao X. Isoflurane promotes non-small cell lung cancer malignancy by activating the Akt-mammalian target of rapamycin (mTOR) signaling pathway. *Med Sci Monit*. 2016;22:4644-4650.
49. Zhang C, Min L, Zhang L, et al. Combined analysis identifies six genes correlated with augmented malignancy from non-small cell to small cell lung cancer. *Tumour Biol*. 2016;37:2193-2207.
50. Bristol ML, Di X, Beckman MJ, et al. Dual functions of autophagy in the response of breast tumor cells to radiation: cytoprotective autophagy with radiation alone and cytotoxic autophagy in radiosensitization by vitamin D 3. *Autophagy*. 2012;8:739-753.
51. Xin Y, Jiang F, Yang C, et al. Role of autophagy in regulating the radiosensitivity of tumor cells. *J Cancer Res Clin Oncol*. 2017;143:2147-2157.
52. Gewirtz DA. An autophagic switch in the response of tumor cells to radiation and chemotherapy. *Biochem Pharmacol*. 2014;90:208-211.
53. Maskey D, Yousefi S, Schmid I, et al. ATG5 is induced by DNA-damaging agents and promotes mitotic catastrophe independent of autophagy. *Nat Commun*. 2013;4:2130.
54. Sorokina IV, Denisenko TV, Imreh G, et al. Involvement of autophagy in the outcome of mitotic catastrophe. *Sci Rep*. 2017;7:14571.
55. Kobayashi D, Oike T, Shibata A, et al. Mitotic catastrophe is a putative mechanism underlying the weak correlation between sensitivity to carbon ions and cisplatin. *Sci Rep*. 2017;7:40588.
56. Mc GMM. Targeting the mitotic catastrophe signaling pathway in cancer. *Mediators Inflamm*. 2015;2015:146282.
57. Gu JJ, Kaufman GP, Mavis C, et al. Mitotic catastrophe and cell cycle arrest are alternative cell death pathways executed by bortezomib in rituximab resistant B-cell lymphoma cells. *Oncotarget*. 2017;8:12741-12753.

How to cite this article: Bai Z, Gao M, Xu X, et al. Overcoming resistance to mitochondrial apoptosis by BZML-induced mitotic catastrophe is enhanced by inhibition of autophagy in A549/Taxol cells. *Cell Prolif*. 2018;51:e12450. https://doi.org/10.1111/cpr.12450